Table 2 Clinical and radiological parameters of RN patients

Case	KPS before BEV therapy	KPS after BEV therapy	Gd-volume size reduction rate (%)	FLAIR-volume size reduction rate (%)	Initial MET L/N	MET L/N ratio reduction rate (%)	Initial CHO L/N	CHO L/N ratio reduction rate (%)
1	60	70	91.2	68.8	2.17	28.2	7.65	84.7
2	90	100	64.8	61.1	2.43	25.3	7.41	67.1
3	60	60	78.1	60.3	2.43	40.7	12.68	63.2
4	70	90	60.6	92.3	2.49	47.6	8.57	79.1
5	90	100	99.0	58.2	1.82	29.7	5.74	63.1
6	60	70	55.9	88.9	2.07	−9.2	20.27	70.8
7	90	100	43.2	65.0	1.91	26.2	7.64	65.7
8	60	60	73.5	25.6	1.89	6.9	4.28	3.5
9	50	70	81.1	64.6	2.50	23.9	8.94	49.2
Mean	70	80	80.0	65.0	2.19	24.4	9.24	60.7

RN radiation necrosis, *KPS* Karnofsky performance status, *BEV* bevacizumab, *Gd* gadolinium, *FLAIR* fluid attenuated inversion recovery, *MET* 11C-methionine, *CHO* 11C-choline, *L/N ratio* lesion/normal tissue ratio

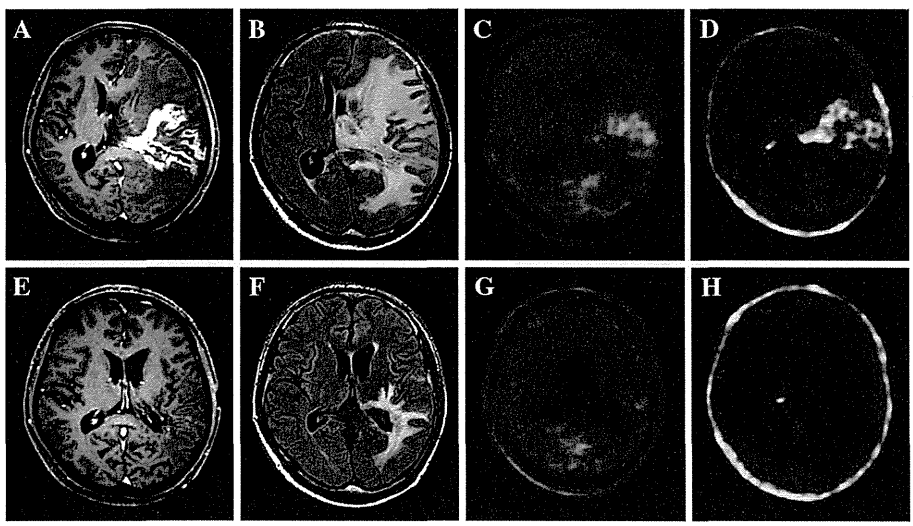

Fig. 1 MRI and PET radiological changes of the Case 1 lesion. An intensive Gd-enhanced lesion (**a**) and extensive abnormal high intensity area on FLAIR (**b**) is seen in the left cerebral hemisphere before BEV therapy. PET demonstrated that the L/N ratio of MET was 2.17 (**c**) and that of CHO was 7.65 (**d**). The Gd-enhanced lesion disappeared (**e**) and the abnormal high intensity area on FLAIR shrunk remarkably (**f**) after BEV therapy. The L/N ratios of MET and CHO substantially decreased to 2.03 (**g**) and 1.17 (**h**) after BEV therapy, respectively

Clinical effects and adverse events

KPS improved in 7 patients (77.8 %) after BEV therapy. Mean KPS scores before and after BEV therapy were 70 and 80, respectively ($p = 0.22$).

BEV-related adverse events of grade 1 or 2 occurred in three patients in which anemia, leukopenia, neutropenia, and lymphocytopenia were observed. High grade adverse effects (more than Grade 3) were not observed. In addition, no indications of previously reported severe adverse events related to BEV treatment, including cerebral hemorrhage or arterial thromboembolic events were observed.

Discussion

Discrimination of RN from tumor recurrence has been a demanding problem in clinical neuro-oncology and is practically important because these two pathologies require different treatments. Traditionally, the only method available to distinguish these two pathologies is histology. Recent advancement of metabolic neuroimaging modalities have made it possible to have a reliable RN diagnosis with both high specificity and sensitivity without tissue examination compared to conventional MRI. RN diagnosed by only neuroimaging (radiological RN) benefits patients since no

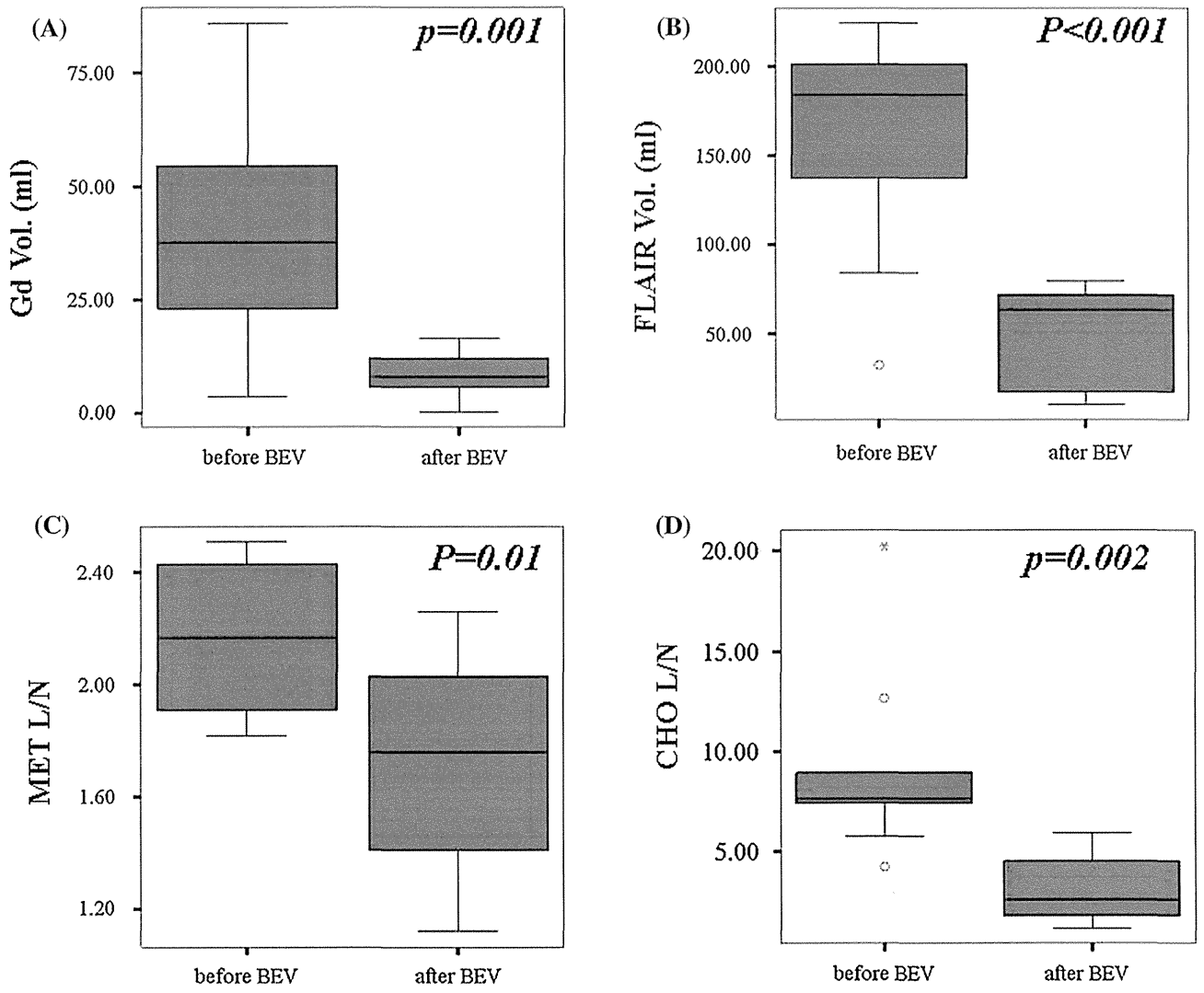

Fig. 2 Box-and-whisker plots outlining the distribution (mean and SD) of the Gd-volume (**a**) and the FLAIR-volume (**b**) of the lesion on MRI before and after BEV therapy, and those outlining the distribution (mean and SD) of the L/N ratios of MET (**c**) and CHO (**d**) of the lesion on PET before and after BEV therapy. The mean values of Gd- and FLAIR-volumes, and MET and CHO L/N ratios significantly decreased after BEV therapy

invasive intervention is then required for diagnosis and subsequent therapeutic decisions, though definitive diagnosis is not always possible with neuroimaging. In addition, there may be some scattered residual tumor cells within or around the RN lesions in cases of malignant gliomas, even if the lesions were reliably diagnosed with RN by histology. In this study, MET-PET was employed for radiological RN diagnosis based on Takenaka et al. [13].

Also in this study, BEV therapy led to a substantial decrease of RN volumes estimated by Gd-MRI and FLAIR and clinical improvements. These results were in agreement with the previous studies by Gonzalez et al. [7] and Levin et al. [8]. The principle therapeutic mechanism of BEV on RN has been thought to be relative normalization of the blood–brain barrier (BBB) attained by decreasing VEGF levels. From this study, another mechanism of BEV impact on RN growth suppression could be due to suppression of RN biological activities from BBB normalization. This proposed mechanism is based on MRS examination in this study and the resulting decrease in tissue metabolism.

Proton MRS is one modern modality for diagnosing and monitoring lesions by evaluating tissue metabolism. Generally, decreased Cho and *N*-acetylaspartate levels and increased lactate and lipid levels are the hallmark of RN [14]. On the other hand, in biologically active RN with progressing mass effect, relatively even Cho levels compared to malignant brain tumors can often be seen [15–17]. In all three cases in which MRS was performed in this study, Cho/Cr ratios were relatively increased before BEV therapy, and significantly decreased after BEV therapy.

Table 3 Multi-voxel proton MRS Cho/Cr ratios of RN

Voxel no.	Case 2		Case 7		Case 9	
	Before	After	Before	After	Before	After
1	7.24	4.53	2.76	1.65	4.82	3.13
2	5.27	3.65	2.94	2.53	4.41	3.76
3	3.75	2.71	5.95	3.11	4.72	4.17
4	6.95	4.23	2.58	1.43	4.94	3.51
5	3.11	2.38	2.87	2.04	2.80	4.05
6	2.07	1.60	8.63	2.37	3.63	3.47
7	3.68	3.29	2.40	1.14	3.84	3.15
8	2.44	2.01	2.50	1.49	3.02	3.07
9	1.79	1.47	3.19	1.62	2.94	2.61
Mean	4.03	2.87	3.76	1.93	3.90	3.44

The Cho/Cr ratios are shown for three cases before and after BEV therapy

Cho/Cr choline/creatine, *BEV* bevacizumab

Such significant reduction of the Cho/Cr ratio cannot be fully explained by BBB normalization. These results suggest that BEV can affect the suppression of tissue biological activity in RN lesions apart from BBB repair.

RN histopathology is characterized as coagulation necrosis induced by vascular damage following irradiation and, later, teleangiectasia, atypia of normal endothelial cells, vascular thickening, vascular proliferation and focal hemorrhage emerge as reactions to tissue hypoxia. Additionally, considerable immunoreactive cells including reactive astrocytes that are attracted to necrotic tissue and lead to granuloma formation often can be seen in RN. Response to radiation is a far more complex and continuous process, consisting of changes in tissue microenvironment, immune cell infiltration, and reparative process modifications [18, 19]. The latter two pathologies are rather strongly related to RN progression and thus, RN is said to be a growing necrotic

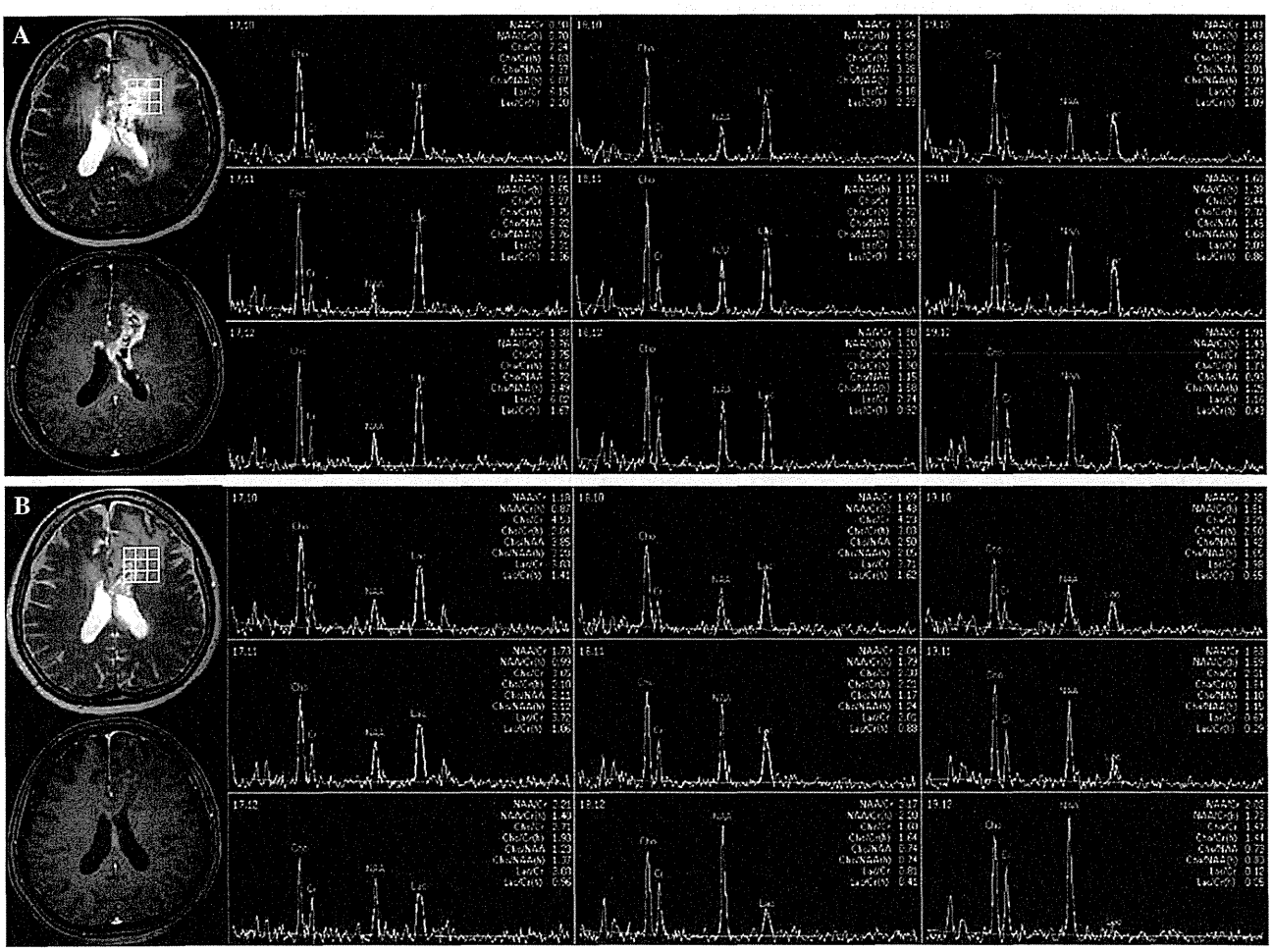

Fig. 3 Changes of multi-voxel MRS of Case 2. Mean Cho/Cr ratio of 9 lesion voxels before BEV therapy was 4.03 (**a**). Cho/Cr ratio of each of the 9 voxels decreased after BEV therapy and the mean Cho/Cr ratio of the 9 voxels also significantly decreased to 2.87 (**b**) after BEV therapy

degeneration. Increased biological activities due to the pathologies are represented as tracer uptake increase in PET as well as Cho/Cr ratio increase in MRS.

The role of PET examination in clinical neuro-oncology is becoming important not only for tumor diagnosis, but also for evaluation of malignancy, invasion, metabolism, and therapeutic effect of brain tumors. In recent PET studies, nonspecific post-therapeutic changes in the brain could be differentiated from tumor-related factors with higher accuracy [1, 20]. In this study, MET- and CHO-PET have been employed for assessing metabolic changes as a result of BEV therapy in RN lesions. In MET-PET, three major factors are likely to affect MET uptake in normal brain tissue as well as in brain lesions. These factors include MET active transport that is responsible for biological activity in tissues, including cell proliferation; passive MET diffusion in regions with BBB disruption; and MET stagnation in regional vascular beds that depend on blood volume. The sum total of MET accumulated through these three mechanisms is regarded as the tissue MET uptake in PET [20–27]. In CHO-PET, however, the mechanism of CHO uptake is thought to be mostly related to passive CHO diffusion, but is not related to active transportation including biosynthesis of phospholipids, which are essential cell membrane components [24]. Therefore, CHO uptake in PET imaging is recognized to be entirely different from the MRS CHO level. Ohtani et al. [28] reported brain tumor imaging with CHO-PET compared with Gd-MRI. They showed that high CHO accumulation areas on PET images were consistent with highly enhanced areas on MR images regardless of brain tumor histopathology, such as pilocytic astrocytoma, meningioma, schwannoma or GBM. Furthermore, the GBM CHO L/N ratio was not necessarily higher than those of other benign brain tumors. Given these findings, CHO accumulation on PET images probably indicates CHO leakage due to BBB disruption as well as lesion enhancement caused by Gd leakage on MRI. Our study showed that disrupted BBB in RN might be repaired by BEV resulting in the decrease of CHO uptake in the same lesions.

In this study, both MET and CHO uptake in RN lesions prominently decreased after BEV therapy. The possible reason for decreased CHO uptake can be attributed to decreased vascular permeability in RN lesions through the effect of BEV. However, considering that the Cho/Cr ratio in MRS was significantly decreased in RN lesions after BEV therapy in this study, decreased MET uptake in RN lesions after BEV therapy indicates a possibility of both decreased vascular permeability and suppressed tissue biological activity, including immunoreactions and inflammation based on BEV effects. Kureshi et al. [29] have reported inflammation, which occurs by radiation-induced injury, and Chiang et al. [30] have explained the mechanism of radiation-induced immunoreactions. Tsuyuguchi et al. [31] have speculated that the accumulation of MET in tissue with radiation injury can be attributed to not only the disrupted BBB and vascularity, but also an inflammatory response. Furthermore, Nordal et al. [5] have reported that expression of hypoxia-inducible factor-1α (HIF1α) and VEGF was seen in association with central nervous system radiation injury. Nonoguchi et al. [6] have reported that immunohistochemistry in RN indicated that HIF1α was expressed predominantly in the perinecrotic area and that a majority of VEGF-expressing cells were reactive astrocytes intensively distributed in this area. Given our findings, we speculate that inflammation in RN may be diminished by BEV resulting in decrease of MET uptake after BEV treatment.

Finally, there is always a risk of misdiagnosis because radiological RN lesions with heterogeneous contrast enhancement may have a mixture of RN and residual tumor cells. Recently, BEV has been used as an anti-cancer agent for inhibition of tumor angiogenesis in malignant gliomas, and a positive clinical effect on survival has been revealed in malignant glioma patients [32–36]. The possibility that the decrease of metabolism in RN lesions as observed in this study may be caused by the anti-tumor effect of BEV on the concomitant residual tumor cells should still be considered. To clarify the issue, studies are needed enrolling limited RN cases more reliably diagnosed using modern neuroimaging.

Conclusions

BEV therapy has been reconfirmed to be a promising therapeutic modality for treating RN both clinically and radiologically. Therapeutic mechanisms of BEV on RN are presumed to be not only BBB repair but also suppression of biological activity such as immunoreactions and inflammation. Further follow-up studies concerning the long term clinical and radiological effects of BEV on RN are needed.

Acknowledgments

Conflict of interest None declared.

References

1. Glantz MJ, Burger PC, Friedman AH, Radtke RA, Massey EW, Schold SC Jr (1994) Treatment of radiation-induced nervous system injury with heparin and warfarin. Neurology 44:2020–2027
2. Kohshi K, Imada H, Nomoto S, Yamaguchi R, Abe H, Yamamoto H (2003) Successful treatment of radiation-induced brain necrosis by hyperbaric oxygen therapy. J Neurol Sci 209:115–117
3. McPherson CM, Warnick RE (2004) Results of contemporary surgical management of radiation necrosis using frameless stereotaxis and intraoperative magnetic resonance imaging. J Neurooncol 68:41–47

4. Presta LG, Chen H, O'Connor SJ, Chisholm V, Meng YG, Krummen L et al (1997) Humanization of an anti-vascular endothelial growth factor monoclonal antibody for the therapy of solid tumors and other disorders. Cancer Res 57:4593–4599
5. Nordal RA, Nagy A, Pintilie M, Wong CS (2004) Hypoxia and hypoxia-inducible factor-1 target genes in central nervous system radiation injury: a role for vascular endothelial growth factor. Clin Cancer Res 15:3342–3353
6. Nonoguchi N, Miyatake S, Fukumoto M, Furuse M, Hiramatsu R, Kawabata S et al (2011) The distribution of vascular endothelial growth factor-producing cells in clinical radiation necrosis of the brain: pathological consideration of their potential roles. J Neurooncol 105:423–431
7. Gonzalez J, Kumar AJ, Conrad CA, Levin VA (2007) Effect of bevacizumab on radiation necrosis of the brain. Int J Radiat Oncol Biol Phys 67:323–326
8. Levin VA, Bidaut L, Hou P, Kumar AJ, Wefel JS, Bekele BN et al (2011) Randomized double-blind placebo-controlled trial of bevacizumab therapy for radiation necrosis of the central nervous system. Int J Radiat Oncol Biol Phys 79:1487–1495
9. Furuse M, Kawabata S, Kuroiwa T, Miyatake S (2011) Repeated treatments with bevacizumab for recurrent radiation necrosis in patients with malignant brain tumors: a report of 2 cases. J Neurooncol 102:471–475
10. Torcuator R, Zuniga R, Mohan YS, Rock J, Doyle T, Anderson J et al (2009) Initial experience with bevacizumab treatment for biopsy confirmed cerebral radiation necrosis. J Neurooncol 94:63–68
11. Miwa K, Matsuo M, Shinoda J, Oka N, Kato T, Okumura A et al (2008) Simultaneous integrated boost technique by helical tomotherapy for the treatment of glioblastoma multiforme with 11C-methionine PET: report of three cases. J Neurooncol 87:333–339
12. Matsuo M, Miwa K, Tanaka O, Shinoda J, Nishibori H, Tsuge Y et al (2012) Impact of [11C]methionine positron emission tomography for target definition of glioblastoma multiforme in radiation therapy planning. Int J Radiat Oncol Biol Phys 82:83–89
13. Takenaka S, Asano Y, Shinoda J, Nomura Y, Yonezawa S, Miwa K, et al (2014) Comparison of 11C-methionine, 11C-choline, and 18F-fluorodeoxyglucose-PET for distinguishing glioma recurrence from radiation necrosis. Neurol Med Chir (Tokyo). 54(4):280–289
14. Shinoda J, Yano H, Ando H, Ohe N, Sakai N, Saio M et al (2002) Radiological response and histological changes in malignant astrocytic tumors after stereotactic radiosurgery. Brain Tumor Pathol 19:83–92
15. Amin A, Moustafa H, Ahmed E, El-Toukhy M (2012) Glioma residual or recurrence versus radiation necrosis: accuracy of pentavalent technetium-99 m-di mercaptosuccinic acid [Tc-99 m (v) DMSA] brain SPECT compared to proton magnetic resonance spectroscopy (H^1-MRS): initial results. J Neurooncol 106:579–587
16. Matoba M, Kondou T, Tanaka T, Kitadate M, Oota K, Tonami H (2010) Noninvasive monitoring of radiation-induced early therapeutic response using high-resolution MR imaging and proton MR spectroscopy in VX2 carcinoma. J Radiat Res 51:690–705
17. Nakajima T, Kumabe T, Kanamori M, Saito R, Tashiro R, Watanabe M et al (2009) Differential diagnosis between radiation necrosis and glioma progression using sequential proton magnetic resonance spectroscopy and methionine positron emission tomography. Neurol Med Chir (Tokyo) 49:394–401
18. Moravan MJ, Olschowka JA, Williams JP, O'Banion MK (2011) Cranial irradiation leads to acute and persistent neuroinflammation with delayed increases in T-cell infiltration and CD11c expression in C57BL/6 mouse brain. Radiat Res 176:459–473
19. Zhao W, Robbins ME (2009) Inflammation and chronic oxdative stress in radiation-induced late normal tissue injury: therapeutic implications. Curr Med Chem 16:130–143
20. Ogawa T, Shishido F, Kanno I, Inugami A, Fujita H, Murakami M et al (1993) Cerebral glioma: evaluation with methionine PET. Radiology 186:45–53
21. Aki T, Nakayama N, Yonezawa S, Takenaka S, Miwa K, Asano Y et al (2012) Evaluation of brain tumors using dynamic ^{11}C-methinone-PET. J Neurooncol 109:115–122
22. De Witte O, Goldberg I, Wikler D, Rorive S, Damhaut P, Monclus M et al (2001) Positron emission tomography with injection of methionine as a prognostic factor in glioma. J Neurosurg 95:746–750
23. Herholz K, Hölzer T, Bauer B, Schröder R, Voges J, Ernestus RI et al (1998) ^{11}C-methionine PET for differential diagnosis of low grade gliomas. Neurology 50:1316–1322
24. Kato T, Shinoda J, Nakayama N, Miwa K, Okumura A, Yano H et al (2008) Metabolic assessment of gliomas using ^{11}C-methionine, ^{18}F-fluorodeoxyglucose, and ^{11}C-choline positron-emission tomography. AJNR Am J Neuroradiol 29:1176–1182
25. Nariai T, Tanaka Y, Wakimoto H, Aoyagi M, Tamaki M, Ishiwata K et al (2005) Usefulness of L-[methyl-11C] methionine-positron emission tomography as a biological monitoring tool in the treatment of glioma. J Neurosurg 103:498–507
26. Ogawa T, Inugami A, Hatazawa J, Kanno I, Murakami M, Yasui N et al (1996) Clinical positron emission tomography for brain tumors: comparison of fludeoxyglucose F 18 and L-methyl-^{11}C-methionine. AJNR Am J Neuroradiol 17:345–353
27. Tovi M, Lilja A, Bergström M, Ericsson A, Bergström K, Hartman M (1990) Delineation of gliomas with magnetic resonance imaging using Gd-DTPA in comparison with computed tomography and positron emission tomography. Acta Radiol 31:417–429
28. Ohtani T, Kurihara H, Ishiuchi S, Saito N, Oriuchi N, Inoue T et al (2001) Brain tumour imaging with carbon-11 choline: comparison with FDG PET and gadolinium-enhanced MR imaging. Eur J Nucl Med 28:1664–1670
29. Kureshi SA, Hofman FM, Schneider JH, Chin LS, Apuzzo ML, Hinton DR (1994) Cytokine expression in radiation-induced delayed cerebral injury. Neurosurgery 35:822–830
30. Chiang CS, McBride WH, Withers HR (1993) Radiation-induced astrocytic and microglial responses in mouse brain. Radiother Oncol 29:60–68
31. Tsuyuguchi N, Sunada I, Iwai Y, Yamanaka K, Tanaka K, Takami T et al (2003) Methionine positron emission tomography of recurrent metastatic brain tumor and radiation necrosis after stereotactic radiosurgery: is a differential diagnosis possible? J Neurosurg 98:1056–1064
32. Friedman HS, Prados MD, Wen PY, Mikkelsen T, Schiff D, Abrey LE et al (2009) Bevacizumab alone and in combination with irinotecan in recurrent glioblastoma. J Clin Oncol 27:4733–4740
33. Kreisl TN, Kim L, Moore K, Duic P, Royce C, Stroud I et al (2009) Phase II trial of single-agent bevacizumab followed by bevacizumab plus irinotecan at tumor progression in recurrent glioblastoma. J Clin Oncol 27:740–745
34. Lai A, Tran A, Nghiemphu PL, Pope WB, Solis OE, Selch M et al (2010) Phase II study of bevacizumab plus temozolomide during and after radiation therapy for patients with newly diagnosed glioblastoma multiforme. J Clin Oncol 29:142–148
35. Narayana A, Gruber D, Kunnakkat S, Golfinos JG, Parker E, Raza S et al (2012) A clinical trial of bevacizumab, temozolomide, and radiation for newly diagnosed glioblastoma. J Neurosurg 116:341–345
36. Vredenburgh JJ, Desjardins A, Herndon JE II, Marcello J, Reardon DA, Quinn JA et al (2007) Bevacizumab plus irinotecan in recurrent glioblastoma multiforme. J Clin Oncol 25:4722–4729

Neurologia medico-chirurgica Advance Publication Date: December 5, 2013

ORIGINAL ARTICLE doi: doi: 10.2176/nmc.oa2013-0117

Comparison of ^{11}C-Methionine, ^{11}C-Choline, and ^{18}F-Fluorodeoxyglucose-PET for Distinguishing Glioma Recurrence from Radiation Necrosis

Shunsuke TAKENAKA,[1] Yoshitaka ASANO,[1,2] Jun SHINODA,[1,2] Yuichi NOMURA,[1] Shingo YONEZAWA,[1] Kazuhiro MIWA,[1] Hirohito YANO,[3] and Toru IWAMA[3]

[1]Chubu Medical Center for Prolonged Traumatic Brain Dysfunction, Kizawa Memorial Hospital, Minokamo, Gifu; Departments of [2]Clinical Brain Sciences and [3]Neurosurgery, Gifu University Graduate School of Medicine, Gifu, Gifu

Abstract

The aim of this study is to assess the different metabolic activities characteristic of glioma recurrence and radiation necrosis (RN) and to explore the diagnostic accuracy for differentiation of the two conditions using ^{11}C-methionine (MET), ^{11}C-choline (CHO), and ^{18}F-fluorodeoxyglucose (FDG)-positron emission tomography (PET). Fifty patients with lesions suggestive of recurrent glioma by MRI underwent MET, CHO, and FDG-PET. All patients who had previously been treated with radiotherapy for malignant glioma were subjected to open surgery and pathological diagnosis (17 recurrent grade 3- gliomas (Gr.3s) comprising 7 anaplastic astrocytomas (AAs) and 10 anaplastic oligodendrogliomas (AOs), 17 recurrent glioblastomas (Gr.4s), and 16 RNs). We measured the PET/Gd volume ratio, the PET/Gd overlap ratio, and the lesion/normal brain uptake ratio (L/N ratio) and determined the optimal index of each PET scan. The PET/Gd volume ratio and the PET/Gd overlap ratio for RN were significantly lower than those of glioma recurrence only with MET-PET ($P < 0.05$). The L/N ratio of RN was significantly lower than that of Gr.4 with all PET imaging ($P < 0.001$) and was significantly lower than that of Gr.3, especially for AO, only with MET-PET images ($P < 0.005$). Receiver operating characteristic (ROC) analysis showed that the area under the curve of MET, CHO, and FDG was 92.5, 81.4, and 77.4, respectively. MET L/N ratio of greater than 2.51 provided the best sensitivity and specificity for establishing glioma recurrence (91.2% and 87.5%, respectively). These results demonstrated that MET-PET was superior to both CHO and FDG-PET for diagnostic accuracy in distinguishing glioma recurrence from RN.

Key words: ^{11}C-methionine, positron emission tomography, radiation necrosis, glioma

Introduction

Radiation necrosis (RN) is a serious clinical complication in the diagnosis and treatment of patients with malignant gliomas. Because the imaging features of most RN appear similar to those of malignant gliomas by computed tomography (CT) or magnetic resonance imaging (MRI), it is difficult to distinguish glioma recurrence from RN. Since therapeutic strategies for these pathological entities are fundamentally different, their differential diagnosis is crucial. Recently, several clinical studies using diffusion MRI,[1–4] perfusion MRI,[3] MR spectroscopy,[3–5] and ^{201}thallium-SPECT[6] have been undertaken in attempts to distinguish between the two conditions. These modalities have made it possible to easily diagnose some cases compared to protocols from the previous era in which only conventional CT or MRI was used. Furthermore, ^{11}C-methionine (MET) and ^{18}F-fluorodeoxyglucose (FDG)-positron emission tomography (PET) have been reported to be more useful for differential diagnosis between glioma recurrence and RN.[6–13] These PET methods were suggested to be superior to other structural neuroimaging modalities from the view-point of feasibility of quantitative evaluation of MET or FDG metabolism in lesions. ^{11}C-choline (CHO) is another tracer candidate which has been

Received April 4, 2013; Accepted June 13, 2013

suggested to be useful for diagnosis of brain tumors in recent PET studies.[14,15]

It is still unclear which PET tracer is best for distinguishing glioma recurrence from RN. We hypothesized that MET-PET is superior to CHO and FDG-PET in this regard, since previous reports have shown the prominent high uptake of CHO may not differentiate non-neoplastic brain lesions with Gd-enhancement from malignant glioma on PET and the high background uptake of FDG in the brain may make it difficult to visually distinguish lesions from normal brain tissue. In this study, the three PET tracers, MET, CHO, and FDG, were compared to determine which PET method was superior for differentially diagnosing glioma recurrence from RN.

Materials and Methods

In this retrospective study from 2002 to 2008, we examined PET scans from 50 consecutive patients with supratentorial space-occupying lesions following radiotherapy for malignant gliomas at the Chubu Medical Center for Prolonged Traumatic Brain Dysfunction, Kizawa Memorial Hospital. All supratentorial space-occupying lesions were Gd-enhanced, and interpretation of the lesions as glioma recurrence or RN was unclear. Presurgical radiologic evaluation was performed with MET, CHO, FDG-PET, and MR imaging in all patients. PET scans and MR imaging were performed in a single day, and the PET images were evaluated using the co-registered MR images. All patients underwent open surgical procedures within 4 weeks after PET scanning, and tumors were classified upon histological examination using the World Health Organisation (WHO) classification system.[16] Of the 50 patients, 17 had recurrent grade 3- glioma (Gr.3), 17 had recurrent glioblastoma (Gr.4), and 16 had RN. The 17 Gr.3s were further classified as 7 anaplastic astrocytomas (AAs) and 10 anaplastic oligodendrogliomas (AOs). RN was pathologically diagnosed in the limited cases in which the surgical specimen showed typical necrotic tissues including thickness and fibrinoid necrosis of the vascular walls, multiple microcysts, coagulation necrosis, endothelial proliferation, and inflammatory cells interspersed with or without scattered tumor cells. The clinical features of the patients are summarized in Table 1. All patients gave written informed consent, and the study protocol was approved by the research committee of the Kizawa Memorial Hospital Foundation.

The PET study was carried out according to standardized procedures recommended by the Japan Radioisotope Association.[17,18] The PET scanner was an ADVANCE NXi Imaging System (General Electric Yokokawa Medical System, Hino-shi, Tokyo), which provided 35 transaxial images at 4.25 mm intervals covering a 25.6 cm in-plane field of view. The in-plane spatial resolution (full width at half maximum) was 4.8 mm, and the scan mode was the standard 2D mode. Before the emission scan was performed, a 3 minute transmission scan was performed to correct photon attenuation with a ring source containing ^{68}Ge. Patients had fasted for at least 4 hours before PET studies. A venous cannula was inserted into the forearm for injection of radiopharmaceuticals. From this cannula, blood samples could also be collected if necessary. A dose of 7.0 MBq/kg of MET, 7.0 MBq/kg of CHO, or 5.0 MBq/kg of FDG was injected intravenously, depending on the particular examination.[17,18] Emission scans were acquired as follows: (1) for 30 minutes, beginning 5 minutes after MET injection, (2) for 7 minutes, beginning 2 minutes after CHO injection, and (3) for 7 minutes, beginning 35 minutes after FDG injection. During PET data acquisition, head motion was continuously monitored using laser beams projected onto ink marks drawn on the forehead and was corrected manually, as necessary. Scan images were reconstructed using the ordered-subsets expectation maximization algorithm (2 iterations, 14 subsets).[19] Images were reconstructed into a 128 × 128 matrix with a pixel size of 2 × 2 mm.

MR imaging was performed with a 1.5 T system (Signa; GE Medical Systems, Milwaukee, Wisconsin, USA). Axial T_1-weighted images (TR/TE/NEX = 350/9/2), T_2-weighted images (2300/100/2), and FLAIR images (800/110/1, inversion time = 2400 ms) (FOV 24 × 24 cm, matrix size 512 × 256) were acquired. The slice thickness was 6 mm, with a 3-mm slice gap. For co-registration of metabolic and anatomic data, 3D spoiled gradient-echo images were also acquired after administration of 0.2 ml/kg of gadopentate dimeglumine (Gd-DTPA) (Magnevist; Nihon Shering, Osaka) using the following parameters: no gap, 1.0 mm thickness, TR/TE = 20.0/1.6 ms, flip angle = 15°, NEX = 1, and axial views.

Tracer accumulation in the regions of interest (ROIs) was analyzed as the standardized uptake value (SUV), which is the activity concentration in the ROI at a fixed time point divided by the injected dose normalized to the patient's measured weight. MET, CHO, and FDG lesion/normal brain uptake ratios (L/N ratios) were calculated by dividing the maximum SUV for the enhanced lesion on the MR image by the mean SUV of the contralateral normal frontal cortex. The lesion SUVs were selected at the highest accumulation, and reference ROIs on each of the three axial planes were drawn with a diameter of 10 mm. Co-registration

Table 1 Summary of clinical features of patients

Pathology	Number of patients	Sex (male: female)	Age (Mean ± SD, y.o.)	Primary tumor pathology (no. of patients)	Primary radiation therapy (no. of patients)	RT dose (Mean ±SD, Gy)	Primary chemotherapy (no. of patients)	Time between RT and this study (Mean ± SD, months)
RN	16	7 : 9	49.1 ± 15.7	AA: 9 AO: 2 GBM: 5	Ex-RT: 8 SRT: 5 Proton therapy + RT: 3	56.1 ± 9.3	TMZ: 8 ACNU + VCR: 2 PCV: 1 CBDCA+VP-16:1 None: 4	28.2 ± 34.4
Gr.3	17	12 : 5	45.7 ± 18.0			53.2 ± 4.4		39.8 ± 41.8
AA	7	6 : 1	45.9 ± 19.2	AA: 7	Ex-RT: 5 SRT: 2	54.6 ± 4.6	TMZ: 1 MCNU: 1 CBDCA+VP-16: 1 None: 4	34.0 ± 49.0
AO	10	6 : 4	45.6 ± 18.1	AO: 10	Ex-RT: 10	52.2 ± 4.2	PCV: 3 MCNU+INF-β: 1 TMZ: 1 None: 5	43.9 ± 38.2
Gr.4	17	7 : 10	42.1 ± 15.6	AA: 7 GBM: 10	Ex-RT: 14 SRT: 2 Proton therapy + RT: 1	60.1 ± 10.2	TMZ: 5 ACNU+VCR: 4 CBDCA+VP-16: 2 None: 6	31.6 ± 42.0

AA: anaplastic astrocytoma, ACNU: nimustine, AO: anaplastic oligodendroglioma, CBDCA: carboplatin, Ex-RT: conventional external radiation therapy, GBM: glioblastoma, Gr.3: recurrent grade 3- glioma, Gr.4: recurrent glioblastoma, INF-β: interferon-β, MCNU: ranimustine, PCV: procarbazine-lomustine-vincristine sulfate therapy, RN: radiation necrosis, RT: radiation therapy, SD: standard deviation, SRT: stereotactic radiotherapy, TMZ: temozoromide, VCR: vincristine sulfate, VP-16: etoposide, y.o.: years old.

of PET and MR imaging was accomplished with an analysis software package (AJS, Tokyo), using the method described by Kapouleas et al.[20] We used the L/N ratio instead of the absolute SUV because of the high, unexplained intersubject variability of the SUV.[21] We used the lesion maximum SUV instead of lesion mean SUV to minimize the effect of lesion heterogeneity. For each PET tracer, we defined regions with L/N ratios greater than 1.5 as PET abnormal high uptake regions and measured the volumes of these regions in each PET image and also the volumes of the Gd-enhanced area in the MRI using an analysis software package (AJS, Tokyo). The volume of the PET abnormal high uptake region overlap with the Gd-enhanced area was measured by the same method for each case. The volume ratio of the PET abnormal high uptake area to Gd enhanced MR area (PET/Gd volume ratio) was calculated as follows: PET/Gd volume ratio (%) = [PET abnormal high uptake area (volume) ÷ Gd-enhanced area (volume)] × 100.

The ratio of the PET abnormal high uptake area overlapping the Gd-enhanced MR area (PET/Gd overlap ratio) was calculated as follows: PET/Gd overlap ratio (%) = [PET abnormal high uptake area overlapping Gd-enhanced area (volume) ÷ Gd-enhanced area (volume)] × 100.

Data are presented as means ± standard deviations (SDs). To compare the L/N ratios of the three PET modalities at the best distinction between glioma recurrence and RN, statistical analysis was performed using analysis of variance and Tukey's test for multiple comparisons. Receiver operating characteristic (ROC) curves were calculated to determine the cut off values for differential diagnosis of glioma recurrence and RN. P values less than 0.05 were considered statistically significant.

Results

I. Volume comparison between MRI and PET studies

The MET-PET/Gd volume ratios of RN, AA, AO, and Gr.4 were 21.7% ± 20.9%, 164.3% ± 158.5%, 185.5% ± 162.6%, and 123.6% ± 66.4%, respectively (Fig. 1A). The MET-PET/Gd overlap ratios of RN, AA, AO, and Gr.4 were 20.7% ± 21.4%, 63.5% ± 40.3%, 74.8% ± 34.0%, and 64.6% ± 29.4%, respectively (Fig. 1D). Both the MET-PET/Gd volume ratio and the MET-PET/Gd overlap ratio of RN were significantly lower than those of AA, AO, and Gr.4, respectively ($P < 0.05$).

The CHO-PET/Gd volume ratios of RN, AA, AO, and Gr.4 were 100.5% ± 20.5%, 110.2% ± 17.3%, 99.9% ± 15.9%, and 104.1% ± 13.7%, respectively (Fig. 1B). The CHO-PET/Gd overlap ratios of RN, AA, AO, and Gr.4 were 83.6% ± 15.1%, 97.4% ± 3.9%, 92.5% ± 10.3%, and 96.1% ± 7.1%, respectively (Fig. 1E). There were no significant differences of the CHO-PET/Gd volume ratios and the CHO-PET/Gd overlap ratios among RN, AA, AO, and Gr.4.

The FDG-PET/Gd volume ratios of RN, AA, AO, and Gr.4 were 0.4% ± 1.5%, 0.5% ± 1.3%, 0.0% ± 0.0%, and 12.1% ± 20.6%, respectively (Fig. 1C). The FDG-PET/Gd overlap ratios of RN, AA, AO, and Gr.4 were 0.4% ± 1.5%, 0.5% ± 1.3%, 0.0% ± 0.0%, and 11.7% ± 19.4%, respectively (Fig. 1F). Both the FDG-PET/Gd volume ratio and the FDG-PET/Gd overlap ratio of Gr.4 were significantly higher than those of RN ($P < 0.05$).

II. Semiquantitative analysis of PET studies

The mean SUVs of MET, CHO, and FDG from the contralateral normal frontal cortex were 1.30 ± 0.25, 0.26 ± 0.94, and 6.31 ± 1.71, respectively. MET L/N ratios of RN, Gr.3, and Gr.4 were 1.95 ± 0.60, 3.40 ± 1.04, and 4.29 ± 1.45, respectively. There was a significant difference between the MET L/N ratios of RN and Gr.3 ($P < 0.005$) and of RN and Gr.4 ($P < 0.001$). However, there was no significant difference between the MET L/N ratios of Gr.3 and Gr.4 (Fig. 2A). MET L/N ratios of AA and AO were 2.79 ± 0.68, and 3.83 ± 1.06, respectively. There was a significant difference between the MET L/N ratios of RN and AO ($P < 0.001$) and AA and AO ($P < 0.05$), but not of RN and AA (Fig. 2D).

CHO L/N ratios of RN, Gr.3, and Gr.4 were 6.90 ± 4.30, 11.18 ± 6.75, and 18.09 ± 10.82, respectively. There was a significant difference only between the CHO L/N ratios of RN and Gr.4 ($P < 0.001$) and of Gr.3 and Gr.4 ($P < 0.05$) (Fig. 2B). CHO L/N ratios of AA and AO were 9.21 ± 4.19, and 12.56 ± 8.01. There was no significant difference between CHO L/N ratios of RN and any of the Gr.3 histological types (Fig. 2E).

FDG L/N ratios of RN, Gr.3, and Gr.4 were 1.15 ± 0.50, 1.26 ± 0.23, and 1.97 ± 0.64, respectively. There was a significant difference only between the FDG L/N ratios of RN and Gr.4 ($P < 0.001$) and of Gr.3 and Gr.4 ($P < 0.001$) (Fig. 2C). FDG L/N ratios of AA and AO were 1.24 ± 0.33, and 1.27 ± 0.16, respectively. There was no significant difference between FDG L/N ratios of RN and any of the Gr.3 histological types (Fig. 2F).

Representative PET and MRI images from RN, AA, AO, and Gr.4 cases are shown in Fig. 3.

III. ROC analysis of PET studies

Fig. 2G shows the ROC curves of the 3 PET modalities. The area under the curve of MET, CHO, and FDG-PETs were 0.925, 0.814, and 0.774,

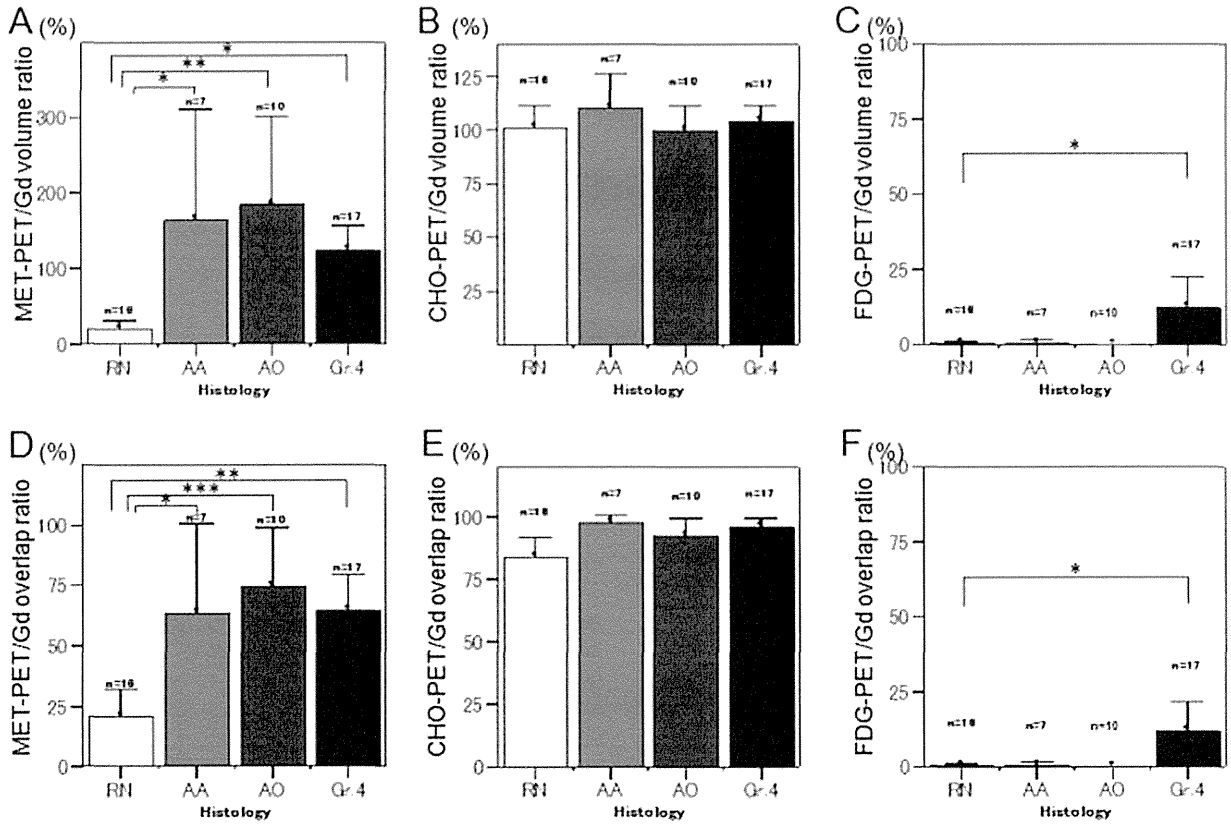

Fig. 1 Graphs showing ^{11}C-methionine (MET)-PET/Gd (A), ^{11}C-choline (CHO)-PET/Gd (B), and ^{18}F-fluorodeoxyglucose (FDG)-PET/Gd (C) volume ratios, and MET-PET/Gd (D), CHO-PET/Gd (E), and FDG-PET/Gd (F) overlap ratios of radiation necrosis (RN), anaplastic astrocytoma (AA), anaplastic oligodendroglioma (AO), and recurrent glioblastoma (Gr.4). The significant low values ($P < 0.05$) of both the PET/Gd volume ratio and the PET/Gd overlap ratio of RN compared with glioma recurrence were shown to be characteristic only for MET-PET. *$P < 0.05$, **$P < 0.005$, ***$P < 0.001$.

respectively. Table 2 shows the best cutoff values, diagnostic sensitivities, and specificities of the 3 PET modalities for recurrent gliomas. The best MET L/N ratio cutoff value was 2.51, which provided a sensitivity of 91.2% and a specificity of 87.5% for diagnosis of glioma recurrence. These results indicate that MET-PET is the most informative method for differentiating tumor recurrence from RN.

Discussion

Radiotherapy has been used for the past four decades as a standard treatment following surgical mass reduction in malignant gliomas. More recently, conventional external radiotherapy has been expanded to include stereotactic radiotherapy, intensity modulated radiotherapy, boron neutron captured therapy, and radiotherapy using heavy ions.[22–25] The usefulness of radiotherapy for malignant gliomas is not in doubt as it has been verified by improved patient survival and local control. However, identifying RN, which deteriorates the clinical condition of patients, is still a critical problem.[26] Normally, 60 Gy of whole brain external irradiation induces necrosis in about 50% of patients up to 5 years after irradiation. Although the therapeutic strategy for RN is different from that for glioma recurrence in most cases of malignant gliomas, it has been difficult to distinguish these pathological entities from each other even using conventional neuroradiological modalities.

With advancements in metabolic neuroimaging, ^{201}thallium-SPECT and FDG-PET have been anticipated to be useful for differential diagnosis between glioma recurrence and Gómez-Río et al. prospectively evaluated ^{201}thallium-SPECT and FDG-PET in 76 patients with suspicion of glioma recurrence after

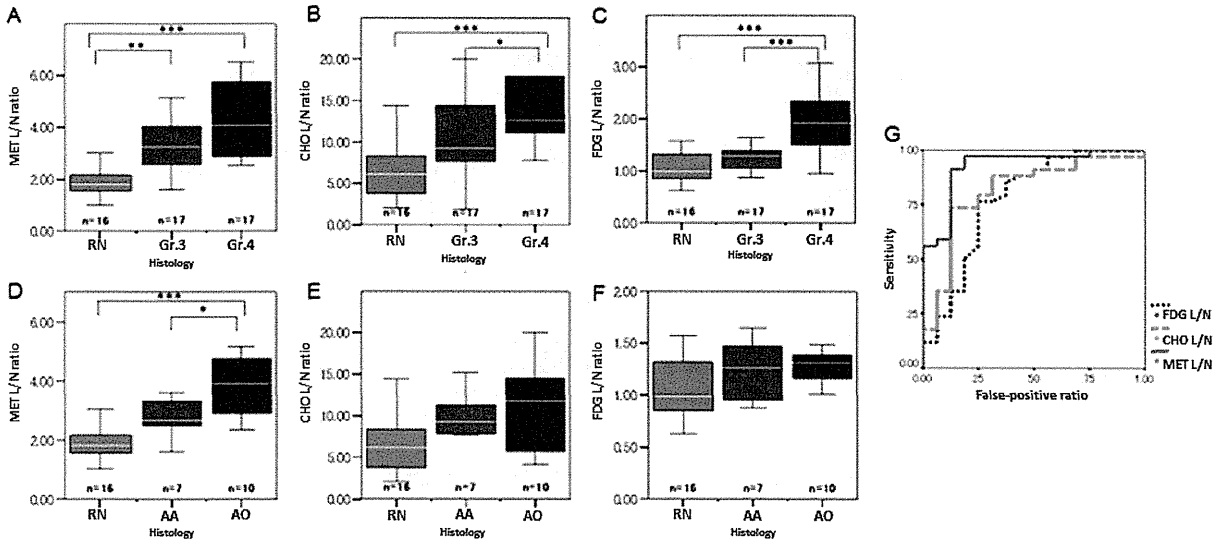

Fig. 2 Graphs showing ^{11}C-methionine (MET) (A), ^{11}C-choline (CHO) (B), and ^{18}F-fluorodeoxyglucose (FDG) (C) lesion/normal brain uptake ratios (L/N ratios) of radiation necrosis (RN), recurrent grade 3- glioma (Gr.3), and recurrent glioblastoma (Gr.4), and MET (D), CHO (E), and FDG (F) L/N ratios of RN, anaplastic astrocytoma (AA), and anaplastic oligodendroglioma (AO). The significant differences of tracer uptake intensity between Gr.4 glioma recurrence and RN were shown in MET ($P < 0.001$), CHO ($P < 0.001$), and FDG ($P < 0.001$) -PETs. Gr. 3 glioma recurrence, especially for AO, could be distinguished from RN only in MET-PET ($P < 0.005$). Graph (G) shows receiver operating characteristic (ROC) curves for the three PET tracers for distinguishing glioma recurrence from RN. The areas under the curve of MET, CHO, and FDG are 0.926, 0.822, and 0.755, respectively. *$P < 0.05$, **$P < 0.005$, ***$P < 0.001$.

surgical excision and radiotherapy.[27] Their results showed that although FDG-PET yielded a slightly higher specificity for diagnosis of glioma recurrence, the sensitivity was considerably lower than that of ^{201}thallium-SPECT. This means that FDG-PET does not clearly improve upon the diagnostic accuracy of ^{201}thallium-SPECT in glioma recurrence.

CHO is another PET tracer recently used for neuroradiological evaluation of gliomas, and it was reported to be a diagnostic agent which was able to differentiate between low-grade gliomas and high-grade gliomas in PET studies, but had not been used for studies of RN.[14] Apart from RN, a high uptake of CHO is also reported in non-neoplastic lesions including brain abscess, inflammatory granulomas, tuberculomas, and some demyelinating diseases which present Gd-enhancement by MRI.[28] A study by Ohtani et al. showed that CHO-PET did not differentiate, in particular, between low-grade gliomas and non-neoplastic lesions.[14] Utriainen et al. described that an association between CHO uptake measured with PET and the concentration of choline containing components measured by 1H-MR spectroscopy was not statistically significant.[29] This data suggests that CHO uptake is scarcely related to intracellular metabolite pools of phosphocholine and glycerophosphocholine.[28] In this study, both the CHO-PET/Gd volume ratio and the CHO-PET/Gd overlap ratio of RN, AA, AO, and Gr.4 were all at levels near 100%. This suggests that there is a regional correspondence between areas of high CHO uptake on PET images and areas with Gd-enhancement on the MRI. These results imply that CHO uptake is mostly dependent on the enhancement effect, which is related to the passive diffusion of materials in regions with BBB disruption, rather than tissue biological activity, which is related to the active transport of materials.

One of the most promising modern neuroimaging protocols in this regard is MET-PET, a popular amino acid imaging modality in oncology indications. MET-PET has been a useful and reliable neuroimaging modality for diagnosis of gliomas because of the correlation of MET-uptake with malignancy and proliferative activity in gliomas and its accumulation during glioma cell invasion.[30,31] Normally, MET uptake is reported to be lower in RN than in glioma recurrence. Tsuyuguchi et al. reported that the mean L/N ratios for RN and glioma recurrence were 1.31 and 1.87.[11] In

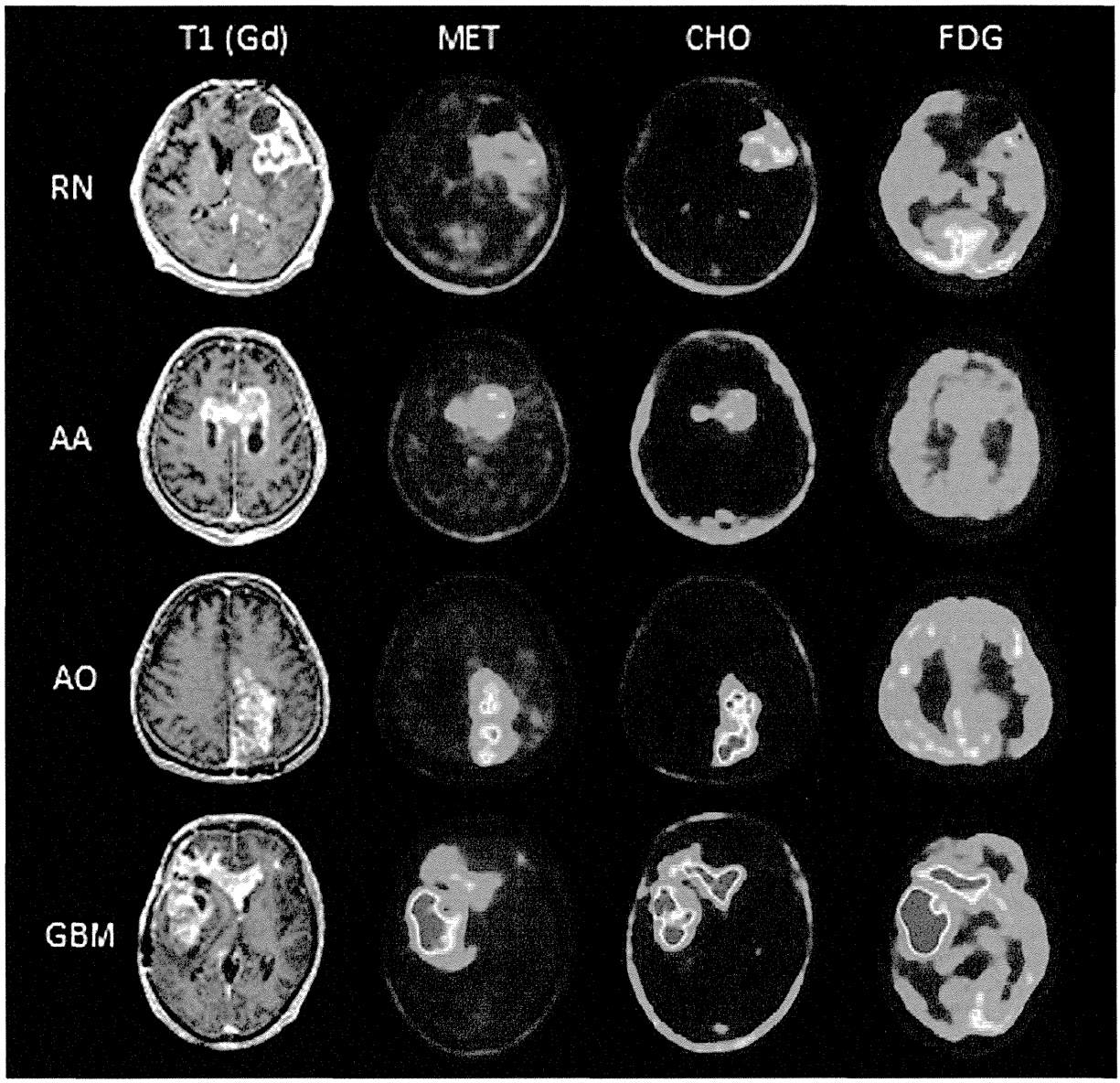

Fig. 3 Representative PET and MRI images of radiation necrosis (RN), anaplastic astrocytoma (AA), anaplastic oligodendroglioma (AO), and glioblastoma (GBM) are shown. RN: A 45-year-old man. ^{11}C-methionine (MET)-PET/Gd volume ratio = 57.0%, MET-PET/Gd overlap ratio = 57.0%, ^{11}C-choline (CHO)-PET/Gd volume ratio = 81.5%, CHO-PET/Gd overlap ratio = 81.5%, ^{18}F-fluorodeoxyglucose (FDG)-PET/Gd volume ratio = 0%, FDG-PET/Gd overlap ratio = 0%, MET lesion/normal brain uptake ratio (L/N ratio) = 3.34, CHO L/N ratio = 2.03, and FDG L/N ratio = 1.57. AA: A 67-year-old man. MET-PET/Gd volume ratio = 189.4%, MET-PET/Gd overlap ratio = 100%, CHO-PET/Gd volume ratio = 121.3%, CHO-PET/Gd overlap ratio = 100%, FDG-PET/Gd volume ratio = 0%, FDG-PET/Gd overlap ratio = 0%, MET L/N ratio = 3.39, CHO L/N ratio = 7.7, and FDG L/N ratio = 1.65. AO: A 51-year-old man. MET-PET/Gd volume ratio = 172.7%, MET-PET/Gd overlap ratio = 100%, CHO-PET/Gd volume ratio = 107.8%, CHO-PET/Gd overlap ratio = 95.3%, FDG-PET/Gd volume ratio = 0%, FDG-PET/Gd overlap ratio = 0%, MET L/N ratio = 5.03, CHO L/N ratio = 14.41, and FDG L/N ratio = 1.31. GBM: A 35-year-old man. MET-PET/Gd volume ratio = 164.9%, MET-PET/Gd overlap ratio = 100%, CHO-PET/Gd volume ratio = 109.2%, CHO-PET/Gd overlap ratio = 98.7%, FDG-PET/Gd volume ratio = 74.3%, FDG-PET/Gd overlap ratio = 67.5%, MET L/N ratio = 5.21, CHO L/N ratio = 17.94, and FDG L/N ratio = 2.33.

Table 2 The best cutoff values and diagnostic accuracy for distinguishing glioma recurrence from RN

Index	Cutoff value	Sensitivity (%)	Specificity (%)
MET L/N	> 2.51	91.2	87.5
CHO L/N	> 8.92	73.5	87.5
FDG L/N	> 1.26	76.5	75.0

CHO: ^{11}C-choline, FDG: ^{18}F-fluorodeoxyglucose, MET: ^{11}C-methionine, L/N: lesion/normal brain uptake, RN: radiation necrosis.

a comparative study, Sonoda et al. showed that MET-PET was superior to ^{201}tallium-SPECT for the differentiation of tumor recurrence from RN.[6] In a comparative study of FDG and MET-PET, van Laere et al. reported that MET was superior to FDG as a diagnostic agent for the evaluation of glioma recurrence because of its higher sensitivity for differentiation from RN.[31]

This is the first study directly comparing the three PET tracers, MET, CHO, and FDG evaluating the diagnostic accuracy in distinguishing glioma recurrence from RN in the same clinical setting. From the ROC analysis of this study, MET-PET was found to be the best of the three tracers in differentiating glioma recurrence from RN with a sensitivity of 91.2% and a specificity of 87.5% with a MET max L/N ratio cutoff value of 2.51. Additionally, only MET-PET could significantly differentiate Gr.3, especially AO, as well as Gr.4 from RN, while FDG and CHO-PET could differentiate only Gr.4 from RN. The L/N ratio cutoff values in this study were relatively higher than that of the previous studies, because L/N ratios were calculated by dividing the maximum SUV for the enhanced lesion on MR imaging by the mean SUV of the contralateral noemal frontal cortex. We used the maximum SUV instead of lesion mean SUV to minimize the effect of lesion heterogeneity.

This study showed the superiority of MET-PET for distinguishing glioma recurrence from RN based on evaluation of intensity of tracer uptake in agreement with previous reports. The significant low values of both the PET/Gd volume ratio and the PET/Gd overlap ratio of RN compared with glioma recurrence were characteristic only with the MET-PET and provide additional evidence for distinguishing glioma recurrence from RN.

The main mechanism for MET accumulation in RN; BBB disruption-related passive diffusion, is presumed to differ from that in tumor recurrence which is active transport affected by cell proliferation. The different mechanisms of MET accumulation for the two pathological processes are the means of potentially distinguishing glioma recurrence from RN by MET-PET. However, because of the substantial tissue biological activity in RN due to cells related to immunological and inflammation reactions and reactive glia cells with a high proliferation potential, some degree of active transport for MET may increase the MET uptake in RN. Additionally, there should be mixed tissues with both RN and residual/recurrent tumor cells around the irradiated region, because it is not feasible to completely kill the malignant glioma cells by clinical irradiation doses. These factors contribute to the continuing difficulty of distinguishing glioma recurrence from RN even using MET-PET in some cases, and further studies for a resolution of this problem are needed.

Recently, 3,4-dihydroxy-6-^{18}F-fluoro-L-phenylalanine (FDOPA) has been utilized as another promising amino acid PET tracer for distinguishing tumor recurrence from RN. Chen et al. reported 98% sensitivity and 86% specificity for the detection of glioma recurrence using FDOPA-PET.[32] 3'-Deoxy-3'-^{18}F-fluorothymicine (FLT) is another recently developed PET tracer for imaging tumor cell proliferation that correlated with Ki-67 values.[33] These tracers appear to be powerful predictors of tumor progression and survival, and comparative studies to evaluate which of the tracers, MET, FDOPA, and FLT, is the most accurate for distinguishing glioma recurrence from RN is needed.

In this study, three PET scans were taken on a single day. This introduced an increase of radiation exposure to patients compared with a single PET scan. "Cross-talk" between PET tracers during subsequent imaging was considered to be minimal, because ^{11}C-labeled tracers such as MET and CHO have short half-lives and sufficient time was allowed between PET scans. However, from this minimal "cross-talk", the order of PET scans (MET, CHO, FDG) could have slightly contributed to our observed result.

MET-PET appears to be superior to both CHO and FDG-PET in diagnostic accuracy for distinguishing glioma recurrence from RN on the basis of intensity as well as extent of tracer uptake volume, and it could play an important role in monitoring newly appearing Gd-enhanced lesions on MRI following radiotherapy in patients with malignant gliomas.

Acknowledgments

The authors thank Prof. Y. Muragaki and Dr. T. Maruyama (Department of Neurosurgery, Tokyo Women's Medical University, Tokyo) for diagnostic suggestions and helpful discussions. They also

thank Mr. S. Fukuyama, Mr. Y. Kasuya, and Mr. R. Okumura (Kizawa Memorial Hospital, Minokamo, Gifu) for technical supports.

Conflicts of Interest Disclosure

The authors have no personal, financial, or institutional interest in any of the drugs, materials, or devices in the article. All authors who are members of The Japan Neurosurgical Society (JNS) have registered online Self-reported COI Disclosure Statement Forms through the website for JNS members.

References

1) Hein PA, Eskey CJ, Dunn JF, Hug EB: Diffusion-weighted imaging in the follow-up of treated high-grade gliomas: tumor recurrence versus radiation injury. *AJNR Am J Neuroradiol* 25: 201–209, 2004
2) Sundgren PC, Fan X, Weybright P, Welsh RC, Carlos RC, Petrou M, McKeever PE, Chenevert TL: Differentiation of recurrent brain tumor versus radiation injury using diffusion tensor imaging in patients with new contrast-enhancing lesions. *Magn Reson Imaging* 24: 1131–1142, 2006
3) Matsusue E, Fink JR, Rockhill JK, Ogawa T, Maravilla KR: Distinction between glioma progression and post-radiation change by combined physiologic MR imaging. *Neuroradiology* 52: 297–306, 2010
4) Rock JP, Scarpace L, Hearshen D, Gutierrez J, Fisher JL, Rosenblum M, Mikkelsen T: Associations among magnetic resonance spectroscopy, apparent diffusion coefficients, and image-guided histopathology with special attention to radiation necrosis. *Neurosurgery* 54: 1111–1117; discussion 1117–1119, 2004
5) Zeng QS, Li CF, Zhang K, Liu H, Kang XS, Zhen JH: Multivoxel 3D proton MR spectroscopy in the distinction of recurrent glioma from radiation injury. *J Neurooncol* 84: 63–69, 2007
6) Sonoda Y, Kumabe T, Takahashi T, Shirane R, Yoshimoto T: Clinical usefulness of ^{11}C-MET PET and ^{201}T1 SPECT for differentiation of recurrent glioma from radiation necrosis. *Neurol Med Chir (Tokyo)* 38: 342–347; discussion 347–348, 1998
7) Patronas NJ, Di Chiro G, Brooks RA, DeLaPaz RL, Kornblith PL, Smith BH, Rizzoli HV, Kessler RM, Manning RG, Channing M, Wolf AP, O'Connor CM: Work in progress: [^{18}F] fluorodeoxyglucose and positron emission tomography in the evaluation of radiation necrosis of the brain. *Radiology* 144: 885–889, 1982
8) Ogawa T, Kanno I, Shishido F, Inugami A, Higano S, Fujita H, Murakami M, Uemura K, Yasui N, Mineura K: Clinical value of PET with 18F-fluorodeoxyglucose and L-methyl-11C-methionine for diagnosis of recurrent brain tumor and radiation injury. *Acta Radiol* 32: 197–202, 1991
9) Kim EE, Chung SK, Haynie TP, Kim CG, Cho BJ, Podoloff DA, Tilbury RS, Yang DJ, Yung WK, Moser RP: Differentiation of residual or recurrent tumors from post-treatment changes with F-18 FDG PET. *Radiographics* 12: 269–279, 1992
10) Ricci PE, Karis JP, Heiserman JE, Fram EK, Bice AN, Drayer BP: Differentiating recurrent tumor from radiation necrosis: time for re-evaluation of positron emission tomography? *AJNR Am J Neuroradiol* 19: 407–413, 1998
11) Tsuyuguchi N, Takami T, Sunada I, Iwai Y, Yamanaka K, Tanaka K, Nishikawa M, Ohata K, Torii K, Morino M, Nishio A, Hara M: Methionine positron emission tomography for differentiation of recurrent brain tumor and radiation necrosis after stereotactic radiosurgery—in malignant glioma. *Ann Nucl Med* 18: 291–296, 2004
12) Terakawa Y, Tsuyuguchi N, Iwai Y, Yamanaka K, Higashiyama S, Takami T, Ohata K: Diagnostic accuracy of ^{11}C-methionine PET for differentiation of recurrent brain tumors from radiation necrosis after radiotherapy. *J Nucl Med* 49: 694–699, 2008
13) Singhal T, Narayanan TK, Jain V, Mukherjee J, Mantil J: 11C-L-methionine positron emission tomography in the clinical management of cerebral gliomas. *Mol Imaging Biol* 10: 1–18, 2008
14) Ohtani T, Kurihara H, Ishiuchi S, Saito N, Oriuchi N, Inoue T, Sasaki T: Brain tumour imaging with carbon-^{11}choline: comparison with FDG PET and gadolinium-enhanced MR imaging. *Eur J Nucl Med* 28: 1664–1670, 2001
15) Kato T, Shinoda J, Nakayama N, Miwa K, Okumura A, Yano H, Yoshimura S, Maruyama T, Muragaki Y, Iwama T: Metabolic assessment of gliomas using ^{11}C-methionine, [^{18}F] fluorodeoxyglucose, and ^{11}C-choline positron-emission tomography. *AJNR Am J Neuroradiol* 29: 1176–1182, 2008
16) Louis DN, Ohgaki H, Wiestler OD, Cavenee WK, Burger PC, Jouvet A, Scheithauer BW, Kleihues P: The 2007 WHO classification of tumours of the central nervous system. *Acta Neuropathol* 114: 97–109, 2007
17) Sub-committee on Medical Application of Cyclotron-Produced Radionuclides, Medical Science and Pharmaceutical Committee, Japan Radioisotope Association: Standards of Compounds Labeled with Positron Nuclides Approved as Established Techniques for Medical Use and Recommendations on Practices of Their Clinical Use (1999 revision). *Radioisotopes* 48: 65-90, 1999
18) Sub-committee on Medical Application of Cyclotron-Produced Radionuclides, Medical Science and Pharmaceutical Committee, Japan Radioisotope Association: Standards of Compounds Labeled with Positron Nuclides Approved as Established Techniques for Medical Use and Recommendations on Practices of Their Clinical Use (Supplement of 1999 Revision). *Radioisotopes* 50: 38–41, 1999
19) Hudson HM, Larkin RS: Accelerated image reconstruction using ordered subsets of projection data. *IEEE Trans Med Imaging* 13: 601–609, 1994
20) Kapouleas I, Alavi A, Alves WM, Gur RE, Weiss DW: Registration of three-dimensional MR and

PET images of the human brain without markers. *Radiology* 181: 731–739, 1991
21) Keyes JW: SUV: standard uptake or silly useless value? *J Nucl Med* 36: 1836–1839, 1995
22) Iuchi T, Hatano K, Narita Y, Kodama T, Yamaki T, Osato K: Hypofractionated high-dose irradiation for the treatment of malignant astrocytomas using simultaneous integrated boost technique by IMRT. *Int J Radiat Oncol Biol Phys* 64: 1317–1324, 2006
23) Narayana A, Yamada J, Berry S, Shah P, Hunt M, Gutin PH, Leibel SA: Intensity-modulated radiotherapy in high-grade gliomas: clinical and dosimetric results. *Int J Radiat Oncol Biol Phys* 64: 892–897, 2006
24) Hermanto U, Frija EK, Lii MJ, Chang EL, Mahajan A, Woo SY: Intensity-modulated radiotherapy (IMRT) and conventional three-dimensional conformal radiotherapy for high-grade gliomas: does IMRT increase the integral dose to normal brain? *Int J Radiat Oncol Biol Phys* 67: 1135–1144, 2007
25) Miyatake S, Kawabata S, Yokoyama K, Kuroiwa T, Michiue H, Sakurai Y, Kumada H, Suzuki M, Maruhashi A, Kirihata M, Ono K: Survival benefit of Boron neutron capture therapy for recurrent malignant gliomas. *J Neurooncol* 91: 199–206, 2009
26) Tanaka Y, Fujii M, Saito T, Kawamori J: [Radiation therapy for brain tumors]. *Nippon Igaku Hoshasen Gakkai Zasshi* 64: 387–393, 2004 (Japanese)
27) Gómez-Río M, Rodríguez-Fernández A, Ramos-Font C, López-Ramírez E, Llamas-Elvira JM: Diagnostic accuracy of ^{201}Thallium-SPECT and ^{18}F-FDG-PET in the clinical assessment of glioma recurrence. *Eur J Nucl Med Mol Imaging* 35: 966–975, 2008
28) Miwa K, Shinoda J, Yano H, Okumura A, Iwama T, Nakashima T, Sakai N: Discrepancy between lesion distributions on methionine PET and MR images in patients with glioblastoma multiforme: insight from a PET and MR fusion image study. *J Neurol Neurosurg Psychiatr* 75: 1457–1462, 2004
29) Utriainen M, Komu M, Vuorinen V, Lehikoinen P, Sonninen P, Kurki T, Utriainen T, Roivainen A, Kalimo H, Minn H: Evaluation of brain tumor metabolism with [^{11}C]choline PET and 1H-MRS. *J Neurooncol* 62: 329–338, 2003
30) Huang Z, Zuo C, Guan Y, Zhang Z, Liu P, Xue F, Lin X: Misdiagnoses of ^{11}C-choline combined with ^{18}F-FDG PET imaging in brain tumours. *Nucl Med Commun* 29: 354–358, 2008
31) Van Laere K, Ceyssens S, Van Calenbergh F, de Groot T, Menten J, Flamen P, Bormans G, Mortelmans L: Direct comparison of 18F-FDG and ^{11}C-methionine PET in suspected recurrence of glioma: sensitivity, inter-observer variability and prognostic value. *Eur J Nucl Med Mol Imaging* 32: 39–51, 2005
32) Chen W, Silverman DH, Delaloye S, Czernin J, Kamdar N, Pope W, Satyamurthy N, Schiepers C, Cloughesy T: 18F-FDOPA PET imaging of brain tumors: comparison study with ^{18}F-FDG PET and evaluation of diagnostic accuracy. *J Nucl Med* 47: 904–911, 2006
33) Chen W, Cloughesy T, Kamdar N, Satyamurthy N, Bergsneider M, Liau L, Mischel P, Czernin J, Phelps ME, Silverman DH: Imaging proliferation in brain tumors with ^{18}F-FLT PET: comparison with 18F-FDG. *J Nucl Med* 46: 945–952, 2005

Address reprint requests to: Yoshitaka Asano, MD, Chubu Medical Center for Prolonged Traumatic Brain Dysfunction, Kizawa Memorial Hospital, 630 Shimo-Kobi, Kobi-cho, Minokamo, Gifu 505-0034, Japan. *e-mail*: yoasano-nsu@umin.ac.jp

J Neurosurg 121:827–838, 2014

Intraoperative cortico-cortical evoked potentials for the evaluation of language function during brain tumor resection: initial experience with 13 cases

Clinical article

Taiichi Saito, M.D., Ph.D.,[1,5,7] Manabu Tamura, M.D., Ph.D.,[1,2,5] Yoshihiro Muragaki, M.D., Ph.D.,[1,2,5] Takashi Maruyama, M.D., Ph.D.,[1,2,5] Yuichi Kubota, M.D., Ph.D.,[1] Satoko Fukuchi, R.T.,[3] Masayuki Nitta, M.D., Ph.D.,[1,2,5] Mikhail Chernov, M.D., D.Med.Sci.,[1,2] Saori Okamoto, M.D.,[2] Kazuhiko Sugiyama, M.D., Ph.D.,[6] Kaoru Kurisu, M.D., Ph.D.,[7] Kuniyoshi L. Sakai, Ph.D.,[4,5] Yoshikazu Okada, M.D., Ph.D.,[1] and Hiroshi Iseki, M.D., Ph.D.[1,2]

[1]Department of Neurosurgery; [2]Faculty of Advanced Techno-Surgery; [3]Central Clinical Laboratory, Tokyo Women's Medical University; [4]Department of Basic Science, Graduate School of Arts and Sciences, The University of Tokyo; [5]CREST, Japan Science and Technology Agency, Tokyo; and Departments of [6]Cancer Chemotherapy and [7]Neurosurgery, Hiroshima University, Hiroshima, Japan

Object. The objective in the present study was to evaluate the usefulness of cortico-cortical evoked potentials (CCEP) monitoring for the intraoperative assessment of speech function during resection of brain tumors.

Methods. Intraoperative monitoring of CCEP was applied in 13 patients (mean age 34 ± 14 years) during the removal of neoplasms located within or close to language-related structures in the dominant cerebral hemisphere. For this purpose strip electrodes were positioned above the frontal language area (FLA) and temporal language area (TLA), which were identified with direct cortical stimulation and/or preliminary mapping with the use of implanted chronic subdural grid electrodes. The CCEP response was defined as the highest observed negative peak in either direction of stimulation. In 12 cases the tumor was resected during awake craniotomy.

Results. An intraoperative CCEP response was not obtained in one case because of technical problems. In the other patients it was identified from the FLA during stimulation of the TLA (7 cases) and from the TLA during stimulation of the FLA (5 cases), with a mean peak latency of 83 ± 15 msec. During tumor resection the CCEP response was unchanged in 5 cases, decreased in 4, and disappeared in 3. Postoperatively, all 7 patients with a decreased or absent CCEP response after lesion removal experienced deterioration in speech function. In contrast, in 5 cases with an unchanged intraoperative CCEP response, speaking abilities after surgery were preserved at the preoperative level, except in one patient who experienced not dysphasia, but dysarthria due to pyramidal tract injury. This difference was statistically significant ($p < 0.01$). The time required to recover speech function was also significantly associated with the type of intraoperative change in CCEP recordings ($p < 0.01$) and was, on average, 1.8 ± 1.0, 5.5 ± 1.0, and 11.0 ± 3.6 months, respectively, if the response was unchanged, was decreased, or had disappeared.

Conclusions. Monitoring CCEP is feasible during the resection of brain tumors affecting language-related cerebral structures. In the intraoperative evaluation of speech function, it can be a helpful adjunct or can be used in its direct assessment with cortical and subcortical mapping during awake craniotomy. It can also be used to predict the prognosis of language disorders after surgery and decide on the optimal resection of a neoplasm.
(http://thejns.org/doi/abs/10.3171/2014.4.JNS131195)

Key Words • **awake craniotomy** • **cortico-cortical evoked potentials** • **surgery** • **brain tumor** • **oncology** • **language function** • **diagnostic and operative techniques**

Surgical removal of intraaxial brain tumors located within or close to language-related cerebral structures represents a significant challenge. To minimize the risk of permanent postoperative speech dysfunction, detailed localization of the frontal language area (FLA) and temporal language area (TLA), as well as their subcortical connections, is critical. At present it can be more or less precisely done with advanced neuroimaging techniques, such as functional MRI,[2,5,12,13,22,29–31,33] diffusion tensor imaging,[4–6,9,22,37] magnetoencephalography,[4] and PET.[4,29] However, the most effective and precise method is direct brain mapping using electrical stimulation, which can be accomplished either after implantation of chronic subdural grid electrodes[4,5,20,21,36,37] or during awake craniotomy.[1,5,6,13,16,22,27,29,31,34,35,37,40]

Abbreviations used in this paper: CCEP = cortico-cortical evoked potentials; ECoG = electrocorticography; FLA = frontal language area; TLA = temporal language area.

Nevertheless, despite its proven effectiveness and widespread acceptance, direct intraoperative brain mapping has some limitations. First, not all patients are suitable for awake craniotomy or can tolerate the procedure.[27,31,37] Second, intraoperative evaluation of the verbal response is generally subjective and can be significantly influenced by the level of consciousness and cooperativeness of the patient, as well as by the parameters of cortical stimulation. Third, negative intraoperative cortical mapping does not fully prevent postoperative deterioration of speech function, which can be observed immediately after surgery in 4%–23% of such cases.[16,34] Fourth, intraoperative evaluation of language can be difficult in patients with a preexisting speech deficit.[22] Fifth, despite the high reliability of intraoperative cortical mapping for anatomical localization of language-related areas, the functional interconnections of these areas generally remain obscured. Sixth, intraoperative mapping of cortical and subcortical structures with electrical stimulation can be performed only at some time points before or between different stages of tumor removal, but is not suitable for constant monitoring during the whole procedure. Finally, while the appearance of durable speech disorders during surgery generally leads to reluctance to perform further tumor resection, the postoperative prognosis of such disorders is hardly predictable. For these reasons, further searches for novel methods of objectively assessing language during awake craniotomy seem reasonable.

The objective in the present study was to evaluate the recording of intraoperative cortico-cortical evoked potentials (CCEP) as an adjunctive method of assessing speech function during the resection of intraparenchymal brain neoplasms. To the best of our knowledge, there have been no previous reports on the application of this neurophysiological technique for brain tumor surgery.

Methods

Between February 2006 and July 2012, intraoperative monitoring of CCEP was applied in 13 patients (11 men and 2 women; mean age 34 ± 14 years) during removal of intraparenchymal brain neoplasms located within or close to language-related structures (FLA, TLA, arcuate fasciculus, and superior longitudinal fasciculus) in the dominant cerebral hemisphere. Detailed characteristics of the patients are shown in Table 1. The ethics committee of the Tokyo Women's Medical University approved the study protocol, and each patient provided informed consent before surgery.

Preoperative Evaluation

Preoperatively 11 of 13 patients had normal language function, whereas mild dysphasia was noted in 2. The neoplasms were predominantly located within the middle or inferior frontal gyrus (6 cases), inferior parietal lobule (4 cases), or insula (3 cases) of the left cerebral hemisphere. In all cases the diagnosis was based on multimodal MRI, which included pre- and postcontrast T1-weighted, T2-weighted, FLAIR, diffusion-weighted, diffusion tensor, and spectroscopic images. Additionally, PET scanning with ^{11}C-methionine, ^{11}C-choline, and ^{18}F-FDG was performed. In all patients the intracarotid amobarbital test revealed that the left cerebral hemisphere was language dominant.

Extraoperative Cortical Mapping

For detailed cortical mapping before tumor removal, 9 of 13 patients underwent subdural implantation of chronic grid electrodes over the cortical area of interest. This technique was usually applied in cases presenting with seizures for precise localization of the epileptic focus relative to the neoplasm and eloquent cortical areas. Each grid (60 × 40 mm) contained 24 electrodes with a diameter of 3 mm and a distance of 10 mm between the centers (Unique Medical Co.). Usually two grids were implanted in each individual to cover a sufficient area of the cortex. Three-dimensional localization of electrodes relative to the brain surface was achieved using Leksell GammaPlan (Elekta Instruments AB), whereas matching of the cortical sulci and gyri was done with BrainVISA software.[38,39] Patients underwent continuous (2–3 weeks) electrocorticography (ECoG) videomonitoring for detection of seizure activity.

Additionally, extraoperative cortical mapping was performed. For this purpose repetitive square wave biphasic current of alternating polarity (pulse width 0.5 msec, frequency 20 or 50 Hz, duration 1–2 seconds) was applied in a bipolar fashion to adjacent pairs of electrodes so that all electrodes were used. Continuous digital ECoG activity was monitored through nonstimulated electrodes to detect seizures and afterdischarges. The stimulus intensity increased steadily from 2 mA using stepwise increments of 1 mA until the effect was attained or abnormalities on ECoG were noted. The maximum stimulus intensity was 6 mA, which corresponds to 12 mA if a monophasic pulse were used. Of note, the maximum stimulus intensity recommended by guidelines of The Japan Awake Surgery Conference[15] for cortical stimulation with the use of subdural electrodes is 16 mA. Cortical stimulations were performed using an Ojemann cortical stimulator (OCS-1, Integra Radionics, Inc.), whereas all recordings were made with a dedicated multimodal neuromonitor (Neuromaster Mee-1000, Nihon Kohden Corp.).

Regions of cerebral cortex were defined as language related if their stimulation consistently interrupted, disturbed, or slowed the patient's ability to name a pictured object, to pronounce a written familiar Japanese word, and/or to generate an action verb during the picture-naming task in the absence of seizures, afterdischarges, and positive and negative motor responses of the tongue (defined as involuntary contraction and impairment of rapid alternating movements, respectively). For confirmation of reproducible results, each cortical area was stimulated at least twice, although never in succession. The testing was recorded on video for subsequent reanalysis.

In our experience, extraoperative cortical mapping significantly reduces the time required for intraoperative localization of eloquent cortical areas (particularly in cases of dominant parietal lobe tumors) and for the overall operation, but cannot substitute for awake craniotomy with direct electrical stimulation particularly aimed at the identification of functionally important subcortical struc-

TABLE 1: Summary of clinical characteristics in 13 patients*

Case No.	Age (yrs), Sex	Tumor Location	Tumor Histology	Type of Anesthesia	Intraop CCEP: Stimulus Intensity (mA)†	Intraop CCEP: Peak Latency (msec)	Intraop CCEP: Direction of Stimulation	Intraop CCEP: Changes During Tumor Removal	% Lesion Resection	Language Function: Preop	Language Function: Intraop	Language Function: Postop Speech Prod Disorder: Presence	Language Function: Postop Speech Prod Disorder: Time to Recovery (mos)
1	35, M	lt middle frontal	AO	local (awake)	6	70	TLA→FLA	unchanged	98	normal	dysarthria	yes‡	1
2	27, M	lt insula	O	local (awake)	8	91	TLA→FLA	disappeared	80	normal	paraphasia, dysarthria	yes	8
3	62, M	lt inferior frontal	AOA	local (awake)	6	90	TLA→FLA	unchanged	30	mild dysphasia	mild dysphasia, similar to preop level	yes, similar to preop level	3
4	12, M	lt middle frontal	CM	general	6	73	TLA→FLA	unchanged	100	normal	NA	no	NA
5	29, M	lt middle frontal	O	local (awake)	6	94	TLA→FLA	unchanged	95	normal	normal	no	NA
6	31, M	lt middle frontal	GBM	local (awake)	6	98	TLA→FLA	unchanged	75	mild dysphasia	mild dysphasia, similar to preop level	yes, similar to preop level	1.5
7	21, F	lt inferior parietal	OA	local (awake)	6	94	FLA→TLA	disappeared	95	normal	paraphasia, repetition failure	yes	10
8	33, M	lt inferior parietal	O	local (awake)	4	66	TLA→FLA	disappeared	95	normal	paraphasia, repetition failure, dysarthria	yes	15
9	26, M	lt insula	AOA	local (awake)	4	94	FLA→TLA	decreased (up to 20%)	85	normal	paraphasia, repetition failure	yes	6
10	41, M	lt insula	O	local (awake)	4	92	FLA→TLA	decreased (up to 40%)§	60	normal	paraphasia, repetition failure	yes	6
11	32, F	lt inferior frontal	AO	local (awake)	4	no response	no response	NA	95	normal	normal	no	NA
12	31, M	lt inferior parietal	AOA	local (awake)	3	80	FLA→TLA	decreased (up to 20%)	95	normal	naming failure, repetition failure	yes	6
13	58, M	lt inferior parietal	AO	local (awake)	6	48	FLA→TLA	decreased (up to 20%)§	40	normal	paraphasia, repetition failure	yes	4

* AO = anaplastic oligodendroglioma; AOA = anaplastic oligoastrocytoma; CM = cavernous malformation; GBM = glioblastoma multiforme; NA = not applicable; O = oligodendroglioma; OA = oligoastrocytoma; Prod = production.

† Electrical stimulus was applied with biphasic current; therefore, actual stimulus intensities are 2 times greater.

‡ Caused by dysarthria due to pyramidal tract injury.

§ In these cases some recovery of CCEP was noted after termination of tumor removal.

tures, such as the arcuate fasciculus and superior longitudinal fasciculus.

Surgery

Surgery was performed according to the previously described concept of the information-guided brain tumor removal, presuming maximum possible resection of the neoplasm with minimal risk of permanent postoperative neurological complications.[23–26] Intraoperative MRI (AIRIS II, Hitachi Medical Corp.), updated neuronavigation, comprehensive neurophysiological monitoring, and detailed histopathological characterization of resected tissue obtained at various stages of the procedure were used routinely. In cases of malignancy, neurochemical guidance of lesion resection with 5-aminolevulinic acid was applied as well. In cases of high-grade gliomas, surgery was generally directed at the maximum possible removal of the contrast-enhanced area visualized on T1-weighted MRI; for low-grade gliomas, surgery was focused on maximum removal of the hyperintense area demonstrated on T2-weighted MRI. Histopathological diagnosis of tumors was based on the current criteria of the WHO.[19]

Intraoperative Brain Mapping

In all but one patient, tumor removal was done during awake craniotomy and was guided by positive mapping of cortical language areas and subcortical structures. These procedures followed dedicated guidelines of The Japan Awake Surgery Conference.[15] Before surgery, patients were familiarized with the tasks used during intraoperative language mapping.[15,37]

For intraoperative brain mapping, electrical stimulation of the cortex was applied with repetitive square wave biphasic current of alternating polarity (pulse width 0.5 msec, frequency 50 Hz, duration 1–2 seconds) using a bipolar electrode probe with an interpolar distance of 5 mm and tip diameters of 1 mm. Stimulation was performed in a systematic manner every 8–10 mm of the cortical surface. Continuous digital ECoG activity was monitored to detect seizures and afterdischarges. The stimulus intensity increased steadily from 2 mA using stepwise increments of 1 mA until the effect was obtained or abnormalities on ECoG were noted. The maximum stimulus intensity was 6 mA, which is in concert with the experience and recommendations of others.[1,5,16,22,34,40] The maximum stimulus intensity in this study corresponded to 12 mA if a monophasic pulse were used, which is in concordance with guidelines of The Japan Awake Surgery Conference.[15] Cortical stimulations were performed using an Ojemann cortical stimulator, and all recordings were done with a dedicated multimodal Neuromaster Mee-1000 neuromonitor.

To demonstrate language assessment tasks to the patient, the dedicated intraoperative examination monitor for awake craniotomy[23,24] was used, which allows real-time visualization, integration and recording of a wide spectrum of data, including a view of the patient's face during response, the type of test provided, the position of the cortical stimulator in the surgical field, and so forth. Cortical stimulation immediately preceded task presentation for the patient and continued for 1–2 seconds.[15] As in extraoperative brain mapping, regions of the cerebral cortex were defined as language-related areas if their stimulation consistently interrupted, disturbed, or slowed the patient's ability to name a pictured object, to pronounce a written familiar Japanese word, and/or to generate an action verb during the picture-naming task in the absence of seizures, afterdischarges, and positive and negative motor responses of the tongue. For confirmation of the reproducible results, each cortical area was stimulated at least 3 times, although never twice in succession. The stimulated sites were initially marked with sterile tags, whereas eloquent cortical areas were delineated with the surgical pen upon the completion of mapping. One centimeter of brain tissue close to the defined borders was preserved during tumor resection. Removal of the neoplasm was accompanied by subcortical stimulation through the resection cavity directed at identifying the language pathways. The devices used for this purpose and the parameters of stimulation, including intensity, were similar to those used for cortical mapping.[15]

During the entire procedure under awake conditions, the patient's ability to speak freely was constantly monitored through continuous conversation with a member of the treatment team who was specialized in assessing language function and provided specific tasks to evaluate recalling, counting, fluency, and comprehension.[37]

Intraoperative CCEP Monitoring

Intraoperative CCEP monitoring was performed continuously before, during, and after tumor resection, with special attention on assessing response during removal of the deep part of the neoplasm adjacent to the arcuate fasciculus and superior longitudinal fasciculus. For this purpose the strip electrodes (diameter 3 mm, distance between centers 10 mm, Unique Medical Co.) were positioned above the FLA and TLA, which were identified with cortical stimulation (Fig. 1). Additionally, recordings through the resection cavity were tried occasionally. Two adjacent electrodes were stimulated in a bipolar fashion with a constant-current square wave of alternating polarity (pulse width 0.3 msec, frequency 1 Hz). Continuous digital ECoG activity was recorded to detect seizures and afterdischarges. The stimulus intensity increased steadily from 2 mA using stepwise increments of 1 mA until the response was attained or abnormalities on ECoG were noted. Actual stimulus intensities in the present study varied from 3 to 8 mA, which is lower than the 10–15 mA used in previous studies of extraoperative CCEP recordings in patients with epilepsy.[4,7,8,21] The reference electrode was placed in the area of the contralateral mastoid process. The bandpass filter for data acquisition was set at 5–1500 Hz with a sampling rate of 5000 Hz for each channel.

In each case the stimulus was applied to the FLA with recordings from the TLA and vice versa, and the CCEP response was defined as the highest observed negative peak in either direction. During each stimulation session two or more trials of 100 responses were averaged using the stimulus onset as the trigger and a delay of 10 msec to

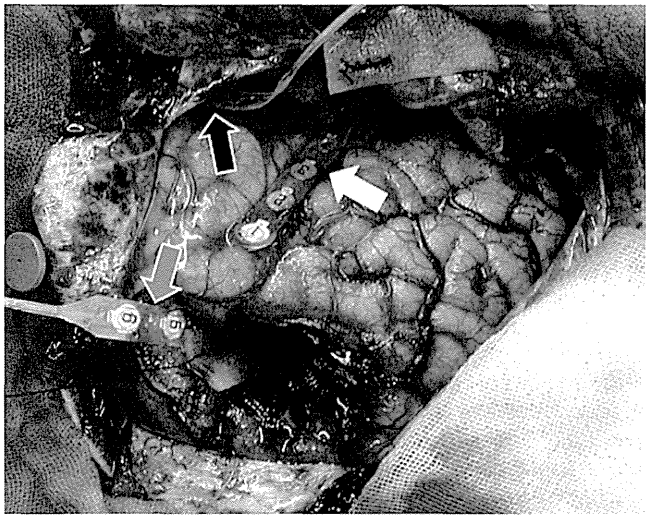

FIG. 1. Case 5. Intraoperative photograph showing strip electrodes for CCEP monitoring, located above the TLA *(black arrow)* and FLA *(white arrow)* and within the resection cavity *(gray arrow)* during removal of the left frontal glioma.

avoid artifacts caused by the stimulation itself. The complete CCEP response was obtained in 100 seconds, but it usually stabilized after the application of 30 stimuli; therefore, the changes, if presented, could be identified in 30–40 seconds. A decrease in the CCEP response was considered to occur when its amplitude reduced approximately 20% or more. All stimulations and recordings of CCEP were performed with a dedicated multimodal neuromonitor (Neuromaster Mee-1000). Patients in the awake condition were not specifically requested to perform any task during CCEP evaluation.

Postoperative Evaluation

Tumor resection rate was assessed with contrast-enhanced MRI performed within 48 hours after surgery. Speech function was evaluated initially after the patient awoke from anesthesia and subsequently on a daily basis until discharge from the hospital. Thereafter all patients were regularly followed up in the outpatient clinic by an attending neurosurgeon. In cases of high-grade gliomas, adjuvant radiochemotherapy was administered as appropriate.

Statistical Analysis

Nonparametric statistical tests were applied to evaluate factors associated with speech disturbances in the early postoperative period and with the time required to recover speech. For statistical analysis, in cases with normal postoperative speech function, the time to speech recovery was considered as 0. Statistical significance was defined at $p < 0.05$.

Results

Intraoperative brain mapping was successfully accomplished in all 12 patients who underwent awake craniotomy. In all cases the FLA and TLA were identified within the posterior part of the inferior frontal gyrus and the posterior part of the superior temporal gyrus, respectively. Additionally, in one patient (Case 13) the middle part of the superior temporal gyrus also contained the TLA.

In 10 of these 12 patients, intraoperative speech dysfunction persisted to the end of surgery. However, in 2 (Cases 3 and 6) of the 10 patients mild dysphasia was present before surgery and was not aggravated during lesion resection, whereas in another patient (Case 1) dysarthria caused by pyramidal tract injury was observed, but dysphasia was not. Among 7 other patients paraphasias and repetition failures were mainly encountered.

An intraoperative CCEP response was not obtained in one patient (Case 11), presumably because of technical problems. In 4 patients (Cases 4 and 6–8) a clear bidirectional response was evident, whereas in 8 others (Cases 1–3, 5, 9, 10, 12, and 13) a definite CCEP response was observed in only one direction. Overall, the best response was identified from the FLA during stimulation of the TLA (7 cases) and from the TLA during stimulation of the FLA (5 cases) with a mean latency of 83 ± 15 msec (range 48–98 msec, median 91 msec). Attempts to detect the CCEP response with strip electrodes located within the resection cavity were not successful in any case.

During removal of the neoplasm the CCEP response was unchanged in 5 cases, decreased (up to 20%–40%) in 4, and disappeared in 3. In all cases changes in the CCEP response abruptly appeared during removal of the deep part of the tumor in the presence of speech dysfunction, but the occurrence of the latter was not always accompanied by alterations in response. In 2 patients (Cases 10 and 13) some recovery of CCEP was noted within 20–30 minutes and was not accompanied by improvement in speech.

Limits for tumor removal were identified through subcortical stimulation of language or motor pathways (Cases 1, 3, 5, 6, and 11), decrease or disappearance of the CCEP response (Cases 7, 8, and 12), or both of these factors (Cases 2, 9, 10, and 13). The median resection rate was 95% (range 30%–100%). Histopathological examination revealed 7 high-grade gliomas, 5 low-grade gliomas, and 1 cavernous malformation. The mean duration of surgery, including two intraoperative MRI sessions, was 8.2 ± 1.7 hours (range 5–10 hours).

Postoperative Course

During the early postoperative period, impairment of speech was noted in 10 of 13 patients. However, as mentioned above, in 2 patients (Cases 3 and 6) the mild dysphasia had been present before surgery and was not aggravated during lesion resection; in another patient (Case 1) dysarthria caused by pyramidal tract injury was observed, but dysphasia was not.

All 7 patients with a decreased or absent CCEP response after tumor removal experienced deterioration in speech function compared with its preoperative level. In contrast, in 5 cases with an unchanged intraoperative CCEP response, including 2 with preexisting mild dysphasia, speaking abilities were preserved at the preoperative level, except in the patient in Case 1, who experienced dysarthria due to pyramidal tract injury. The difference